J Ginseng Res 44 (2020) 105–114

Contents lists available at ScienceDirect

Journal of Ginseng Research

journal homepage: http://www.ginsengres.org

Research Article

Putative multiple reaction monitoring strategy for the comparative pharmacokinetics of postoral administration Renshen–Yuanzhi compatibility through liquid chromatography–tandem mass spectrometry

Yufei Sun [1,2], Guifang Feng [1,2], Yan Zheng [1], Shu Liu [1,*], Yan Zhang [3], Zifeng Pi [1], Fengrui Song [1], Zhiqiang Liu [1,*]

[1] State Key Laboratory of Electroanalytical Chemistry, National Center of Mass Spectrometry in Changchun, Jilin Province Key Laboratory of Chinese Medicine Chemistry and Mass Spectrometry, Changchun Institute of Applied Chemistry, Chinese Academy of Sciences, Changchun, China
[2] University of Science and Technology of China, Hefei, China
[3] School of Chemical and Pharmaceutical Engineering, Jilin Institute of Chemical Technology, Jilin, China

ARTICLE INFO

Article history:
Received 8 May 2018
Received in Revised form
25 August 2018
Accepted 28 September 2018
Available online 9 October 2018

Keywords:
Herb–herb interactions
Liquid chromatography coupled with mass spectrometry
Pharmacokinetics study
Radix Ginseng
Radix Polygala

ABSTRACT

Background: Exploring the pharmacokinetic (PK) changes of various active components of single herbs and their combinations is necessary to elucidate the compatibility mechanism. However, the lack of chemical standards and low concentrations of multiple active ingredients in the biological matrix restrict PK studies.

Methods: A putative multiple reaction monitoring strategy based on liquid chromatography coupled with mass spectrometry (LC–MS) was developed to extend the PK scopes of quantification without resorting to the use of chemical standards. First, the compounds studied, including components with available reference standard (ARS) and components lacking reference standard (LRS), were preclassified to several groups according to their chemical structures. Herb decoctions were then subjected to ultrahigh-performance liquid chromatography coupled with quadrupole time-of-flight mass spectrometry analysis with appropriate collision energy (CE) in MS^2 mode. Finally, multiple reaction monitoring transitions transformed from MS^2 of ultrahigh-performance liquid chromatography coupled with quadrupole time-of-flight mass spectrometry were used for ultrahigh-performance liquid chromatography coupled with triple quadrupole mass spectrometry to obtain the mass responses of LRS components. LRS components quantification was further performed by developing an assistive group-dependent semiquantitative method.

Results: The developed method was exemplified by the comparative PK process of single herbs Radix Ginseng (RG), Radix Polygala (RP), and their combinations (RG–RP). Significant changes in PK parameters were observed before and after combination.

Conclusion: Results indicated that Traditional Chinese Medicine combinations can produce synergistic effects and diminish possible toxic effects, thereby reflecting the advantages of compatibility. The proposed strategy can solve the quantitative problem of LRS and extend the scopes of PK studies.

1. Introduction

One of the characteristics of Traditional Chinese Medicine (TCM) treatment is combination therapy [1]. Compared with individual herbs or single active ingredients used alone, TCM formulae containing multiple herbs as entirety offer better therapeutic efficacies [2]. In recent years, studies have gradually shifted from monosubstance therapy toward combination therapies [3]. Multiple therapies are expected to present vigorous vitality in clinical practices and drug discoveries. Therefore, lucubrate of the

* Corresponding authors. Changchun Institute of Applied Chemistry, Chinese Academy of Sciences, 5625 Renmin Street, Changchun 130022, Jilin, China.
E-mail addresses: mslab20@ciac.ac.cn (S. Liu), liuzq@ciac.ac.cn (Z. Liu).

https://doi.org/10.1016/j.jgr.2018.09.007
p1226-8453 e2093-4947/$ – see front matter

interactions of multiple components among corresponding herbs is necessary to modernize TCM. The first step in elucidation is to understand the compatibility of the two herbs.

The absorption, distribution, metabolism, and elimination of active ingredients might change significantly after the compatibility of the given herbs is compared with that of the single herbs [4]. Pharmacokinetics (PK) was applied to investigate the compatibility of the herbs [5–7]. In addition, elaboration of the dynamic process of multicomponents in a complex matrix *in vivo* is required for drug development and clinical monitoring. The multiple reaction monitoring (MRM) modes on ultrahigh-performance liquid chromatography coupled with triple quadrupole mass spectrometry (UHPLC–TQ MS) have been perceived to be the most reliable method for quantitative analysis owing to its high sensitivity, precision, and accuracy based on standards [2,8].

In spite of the powerful capabilities in the quantification of the MRM by UHPLC–TQ MS, the following issues remain unresolved when it was used to study *in vivo* the pharmacokinetics of multicomponents. Plasma matrices are usually complicated, and thus, trace constituents are difficult to detect. In addition, the challenges such as the lacking reference standards in the quantitative aspect seem to be even greater. As a thoroughly researched herb, Radix Ginseng (RG) has abundant commercially available reference standards for PK study, while lacking pure standards for Radix Polygala (RP) proved to be a mortal blow for our holistic PK study [9,10]. To address this problem, several attempts have been made to predict the optimal CE for peptide empirically [11,12] or infer precursor–product pairs of metabolites according to a program written in advance [13,14]. Nevertheless, these approaches may not be applicable for active phytochemical constituents of herbs because of the diverse structure and property between them. In this study, a strategy has been proposed for optimizing MRM transitions and corresponding parameters online independent of reference standards (Fig. 1). The MRM transitions and the corresponding parameters of those RG and RP components with available reference standard (ARS) were conveniently gained by individually injecting the standards into the ion source using conventional protocols [15,16], whereas the MRM transitions and the corresponding parameters of those RP compounds with lacking reference standard (LRS) were optimized online as follows. First, the RP compounds were preclassified into several groups according to their chemical structures. Subsequently, samples of RP decoction were subjected to UHPLC–Q–TOF MS analysis with appropriate CE. Finally, MRM transitions transformed from the MS^2 of UHPLC–Q–TOF MS were used for UHPLC–TQ MS to obtain the mass responses of the components.

The proposed strategy was applied on the comparative PK study of monoherbs RG and RP and the herb pair RG–RP with a weight ratio of 3:2 to monitor the variations before and after combinations. The herb pair is widely used in many TCM formulae, such as Ding-Zhi-Xiao-Wan, YuanZhi-Wan, and RenShen-YuanZhi-San [17]. RG shows beneficial antiinflammatory, age defying, and immune dysfunction effects [18]. RP plays an important role in the treatment of insomnia, depression, and so on [2,19]. They have complementary pharmacological effects in the therapy of senile diseases. However, the PK behavior deciphering the interaction characteristics of multicomponent process *in vivo* has not been reported until now. Protopanaxadiol (PPD)-type ginsenoside (Rb1, Rb2, Rb3, Rc, and Rd), protopanaxatriol (PPT)-type ginsenoside (Rg1, Re, and Rf) of RG and xanthone [polygalaxanthone III (PIII) and sibiricaxanthone A (Sibi A)], sucrose esters [sibiricose A5 (SA5), sibiricose A6 (SA6), 3,6-disinapoyl sucrose (3,6-D), tenuifoliside A (Ta), tenuifoliside B (Tb), and tenuifoliside C (Tc)], and triterpene saponins tenuifolin (Tf) were the main active ingredients according to our laboratory's previous work [20,21]. The chemical structures of those components mentioned and dioscin, which is an internal standard (IS), are shown in Fig. S1. In this study, we have comprehensively monitored the variations of the dynamic processes of the ingredients mentioned in the herb pair by the established method.

2. Experimental design

2.1. Materials and reagents

RG and RP were purchased from Fusong Shenchang of Jilin province (Jilin, China) and Hebei Kaida Traditional Chinese Medicine Co. Ltd (Hebei China), respectively. All herb medicines were identified by Professor Shumin Wang (Changchun University of Chinese Medicine). The reference standards of ginsenosides, namely, Rb1, Rb2, Rb3, Rc, Rd, Rg1, Re, and Rf, were obtained from the College of Pharmacy of Jilin University, and the RP reference standards, namely, polygalaxanthone III, sibiricoses A6, 3,6-Disinapoyl sucrose, tenuifoliside A, and tenuifolin, were obtained from the Purification Engineering Technology Research

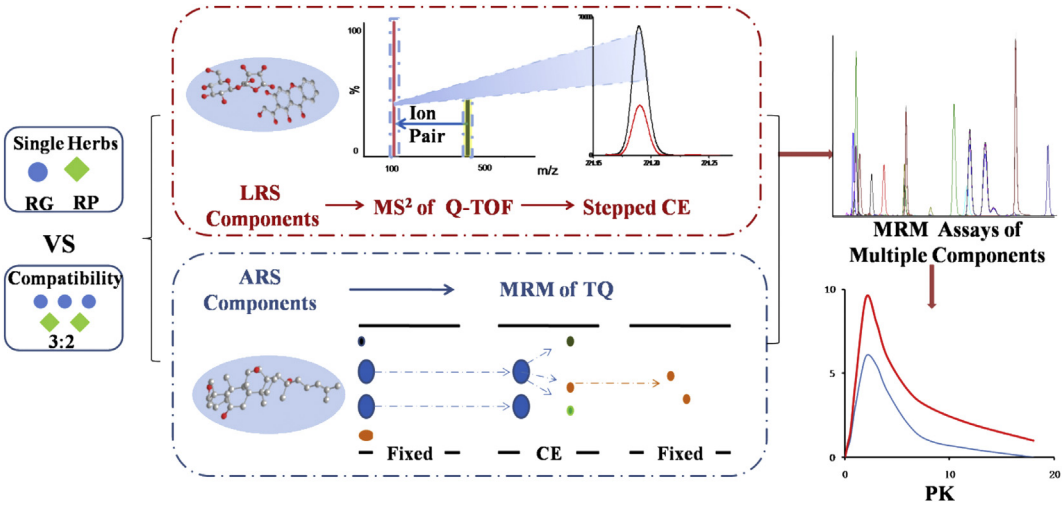

Fig. 1. Strategy proposed for comprehensive quantification of active components. The red dotted line box represents the optimized process of components with LRS, whereas the blue dotted line box represents the optimized process of components with ARS. ARS, available reference standard; CE, collision energy; LRS, lacking reference standard; MRM, multiple reaction monitoring; PK, pharmacokinetic; RG, Radix Ginseng; RP, Radix Polygala; Q-TOF, quadrupole time of flight.

Center of Sichuan Province Natural Medicine (Sichuan, China). Diosin was purchased from the Quality Inspection Center of China. HPLC-grade acetonitrile, methanol, and formic acid were obtained from Fisher Scientific (Loughborough, UK). The analytical-grade reagents, isopropyl alcohol, acetone, and n-butanol were provided by Beijing Chemical Works (Beijing China). The deionized water was prepared using Milli-Q water (18.2 MΩ) purification system (Milford, MA, USA).

2.2. Preparation of herb decoctions

RG–RP decoction was prepared as follows: 90 g of RG powder and 60 g of RP powder were immersed in 1.2 L of 75% ethanol aqueous solution for 1 h and then refluxed 2 times, each for 2 h. The combined ethanol extracts were filtered with gauze to remove solids and then concentrated by rotary evaporation under vacuum to a certain volume. The concentrate was lyophilized to obtain the powder extract. These powders were dissolved again in water and administrated orally to rats. Meanwhile, the single-herb decoction of RG and RP were prepared by the preparation method for RG–RP decoction and administrated proportionally.

2.3. Preparations of sample solutions

All samples (−20°C) were thawed at room temperature. Then, 10 μL of IS solution (1 μg mL^{-1}) was added to 100 μL of plasma sample and homogeneously mixed before processing. The mixture was extracted with 0.8 mL of MET-n-BUT (4:1; −20°C) for 10 min. The upper layer was centrifuged at 14000 rpm for 10 min and dried under N_2 for approximately 40 min at 45°C. The residues were then redissolved in 100 μL of methanol–water (1:1, v/v) solution and consequently centrifuged at 14000 rpm for 10 min.

2.4. Preparation of standard solutions

Stocking solutions of 1 mg mL^{-1} for all standards and IS were obtained by dissolving the precisely weighed powders in a corresponding volume of methanol. Working solutions were freshly diluted with methanol. Consequently, 10 μL of each working solution was spiked into 90 μL of blank plasma to obtain the concentrations of 2.5, 5, 10, 25, 50, 100, 250, 500, 1000, 5000, and 10000 ng mL^{-1} for the calibration curve. The quality control samples were prepared at three concentration levels of 10, 100, and 1000 ng mL^{-1}. The concentration of IS was set at 100 ng mL^{-1}. The calibration curve and quality control samples were pretreated by the procedure similar to that of the sample solution mentioned in Section 2.2.

2.5. Instruments and chromatographic conditions

Waters Acquity UHPLC system (Waters Corp, USA) combined with a Q-TOF SYNAPT G2 mass spectrometer was used to obtain the MS^2 data. Data were acquired through continuous negative ionization mode. The optimized parameters were as follows: the source temperature was 110°C, and the desolvation gas temperature was 300°C. The flow rates of cone and desolvation gas were set at 50 and 600 L h^{-1}, respectively. The voltages of capillary, cone, and extraction cone were set at 2.0 kV, 25 V, and 4.0 V, respectively. Leucine enkephalin was used as a lock mass compound with a reference mass at m/z 554.2615 in the negative ion mode. The data were acquired using MassLynx software 4.1 (Waters Corp, USA).

A Shimadzu UHPLC system (Shimadzu, Japan) combined with a 8050 triple quadrupole mass spectrometer (Shimadzu, Japan) was used to acquire the quantitation data. The optimum parameters are as follows: nebulizing gas flow, 3.0 L min^{-1}; drying gas flow, 10.0 L min^{-1}; heating gas flow, 10.0 L/min; Electronic Spray Ion (ESI) interface voltage, 3.0 kV; interface temperature, 300°C; Desolvent Line (DL) temperature, 250°C; Ion Gauge (IG) vacuum, 4.4e−4 Pa; and Pilani vacuum Gauge (PG) vacuum, 150 Pa. Dwell and pause times were both set as 5 ms. Data acquisition was performed using LabSolution LCMS ver. 5.6 software (Shimadzu, Japan).

Shield RP18 Column (2.1 × 50 mm, 1.7 μm) was used to conduct chromatographic separation at 40°C, and a flow rate of 0.3 mL min^{-1} was maintained. A sample injector (4°C) was used to inject 10 μL of each sample into the system. Water with 0.1% formic acid (A) and acetonitrile (B) was used as the mobile phase. The optimum gradient program conditions are as follows: 0–1 min, 10–19% B linear; 1–6 min, 19% B isocratic; 6–6.5 min, 19–28% B linear; 6.5–16 min, 28% B isocratic; 16–18 min, 28–45% B linear; 18–23 min, 45% B isocratic; 23–24 min, 45–100% B linear; and 24–25 min, 100% B isocratic.

3. Method validation

The proposed method was validated according to the Food and Drug Administration guidelines for bioanalytical method validation [22–24]. Specificity, linearity, sensitivity, etc. were investigated comprehensively. The detailed experimental scheme is described in the supporting information.

3.1. PK study

Sprague–Dawley (SD) rats (male, weighing 300 ± 20 g) were supplied by Dalian Medical University (Dalian, China). Standard laboratory conditions (temperature, 25 ± 2°C; humidity, 50% ± 5%) were prepared for rats, and they were accommodated for one week with adequate food and water. The rats were fasted overnight and only provided access to water before the PK study. All the experimental procedures were performed in accordance with the Guide for the Care and Use of Laboratory Animals.

Eighteen rats were randomly divided into three groups (six rats per group). After oral administration of GS–RP extract at a dosage of 12.5 g kg^{-1}, GS extract at a dosage of 7.5 g kg^{-1}, and RP extract at a dosage of 5 g kg^{-1} to rats, approximately 0.5 mL of blood samples was collected from the suborbital vein into heparinized tubes before and 0.25, 0.5, 0.75, 1, 2, 4, 6, 8, 12, 24, 36, and 72 h after dosing. The plasma sample was harvested by centrifugation at 5000 rpm for 10 min and then stored at −20°C.

4. Results and discussion

4.1. Optimization of the extraction procedure

One of the obstacles to of the analysis of multiple trace compounds in plasma samples is the sample pretreatment owing to the low concentration, high level of noise, and different polarities. In the present study, different methods of extraction, such as protein precipitation, liquid–liquid extraction, and solid phase extraction, were considered to obtain high recoveries of analytes and low interference at the same time [22–24]. As shown in Table S1, solid phase extraction with problems such as multiple operation steps, low efficiency, and time consumption cannot satisfy the necessity for large quantities of test samples for PK studies. For protein precipitation and liquid–liquid extraction, three factors were considered: proper extraction agent (methanol, acetonitrile, acetone, isopropanol, and n-butyl alcohol), temperature, and volume of the extraction agent. After extraction, none of them can provide high recovery for all the components. Even so, methanol and n-butyl alcohol play complementary roles for some components (3,6-D, Ta, Tf, PIII, and so on) in the premise of high recovery of the other components (Rb1, Rb2, Rb3, Rc, Rd, etc.) (Table S1). Accordingly, we speculated that the methanol and n-butyl alcohol mixture can be a

satisfactory precipitating agent, with all of the components obtaining higher extraction recovery. According to Table S2, MET-n-BUT (4:1) was found to be the best due to its relatively high extraction recovery for analytes. In addition, the volume (0.6, 0.8, and 1.0 mL) and temperature (−80, −20, and 20°C) have significance influence on the extraction efficiency. Finally, 0.8 mL of organic solvents (−20°C) was used.

4.2. Optimization of HPLC conditions

Given that the structural similarity of the components of partial compound in RG–RP compatibility even with some isomers, optimization of the HPLC condition is vital. The chromatographic conditions were obtained after a stepwise optimization to obtain the proper separation and elevate the mass response of components simultaneously. Finally, the 18 components including some structural isomers were separated on a BEH shield RP column with acetonitrile–water as the mobile phase. Moreover, the addition of 0.1% formic acid to the solvent obviously improved the peak shape and increased the signal response. The representative extracted ion chromatograms acquired from mixed standard solutions are shown in Fig. 2.

4.3. MRM transitions putative from MS^2

MRM optimization is always constructed by direct infusion of reference standards into the ion source of TQ-MS; hence, the coverage is largely restricted by commercial available standards. Compared with UHPLC–TQ MS, UHPLC–Q–TOF MS is capable of recording fragment ions on MS^2 mode independent of reference standards [14,25,26]. To broaden the coverage of MRM, we developed an online putative MRM (PMRM), in which major MS parameters were derived from MS^2 of UHPLC–Q–TOF MS. First, the nine RP components were classified into three groups, in which the components with LRS exhibited similar chemical structure to those with ARS (Fig. 3). The similarity of the chemical structures can guarantee similarity in polarity, chromatographic behaviors, and fragmentation rules. This guarantees accurate determination of the MRM transitions of components with LRS. Second, for components with standards, optimum MRM transitions and corresponding parameters were obtained by infusing reference standards into the ion source of the TQ-MS (Table S3). Meanwhile, the same standards were fragmented with Q-TOF in MS^2 mode to obtain precursor/product ion pairs (Fig. 4 A, C and Fig. S2 A, C). Comparing the daughter ions optimized from UHPLC–TQ MS with the fragmentation ions obtained from UHPLC–Q–TOF MS, similar fragmentation modes can be conformed among instruments with different vendor. Then, the extract of RP was infused into the ion source of the Q-TOF to fragment in MS^2 mode to obtain precursor/product ion pairs for the components with LRS (Fig. 4 B, D and Fig. S2 C, D). Comparing the fragmentation rules of the same group components, nearly the same fragmentation rules exist in components with similar chemical structures. Finally, based on the aforementioned precondition,

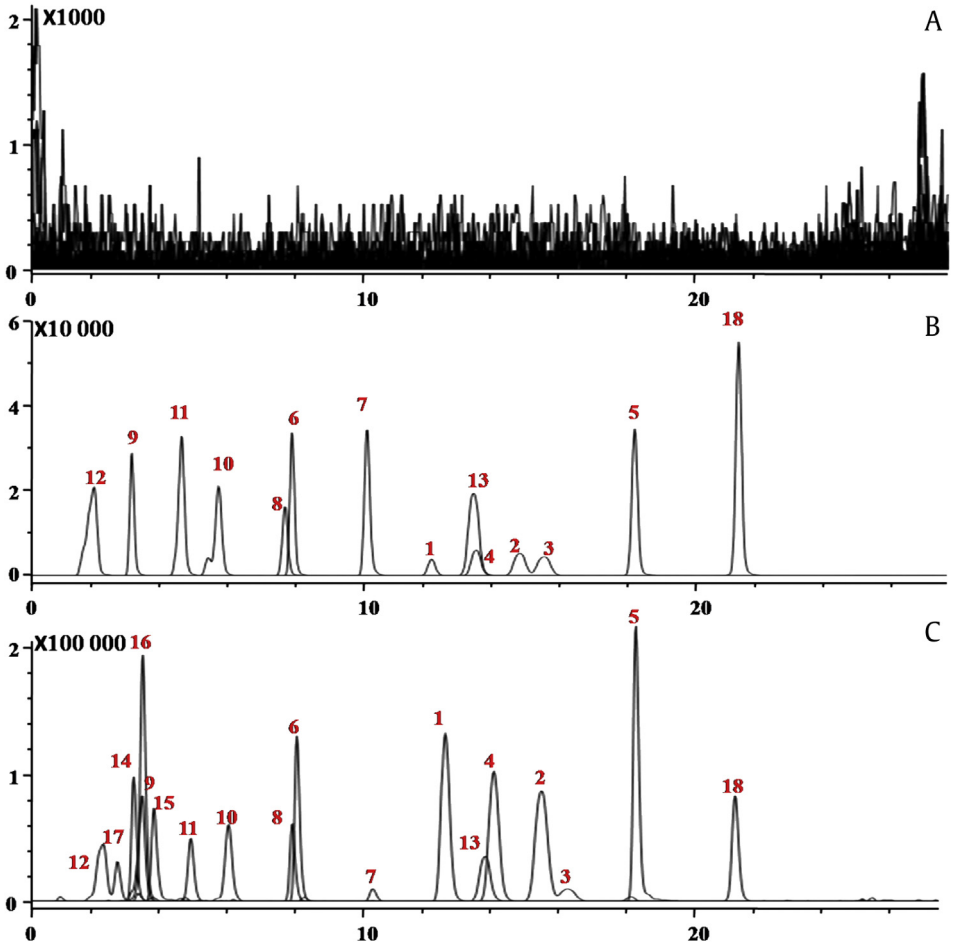

Fig. 2. Representative MRM chromatograms for drug-free rat plasma and rat plasma spiked with active components and IS. (A) MRM chromatogram of blank rat plasma. (B) MRM chromatogram of blank plasma spiked with 13 reference standards and IS. (C) MRM chromatogram of rat plasma collected at 1 h after i.g. administration of RG–RP extract. (1, Rb1; 2, Rb2; 3, Rb3; 4, Rc; 5, Rd; 6, Re; 7, Rf; 8, Rg1; 9, PIII; 10, Ta; 11, 3,6-D; 12, SA6; 13, Tf; 14, Sibi A; 15, Tb; 16, Tc; and 17, SA5). i.g., intragastrical administration; IS, internal standard; MRM, multiple reaction monitoring; RG, Radix Ginseng; RP, Radix Polygala.

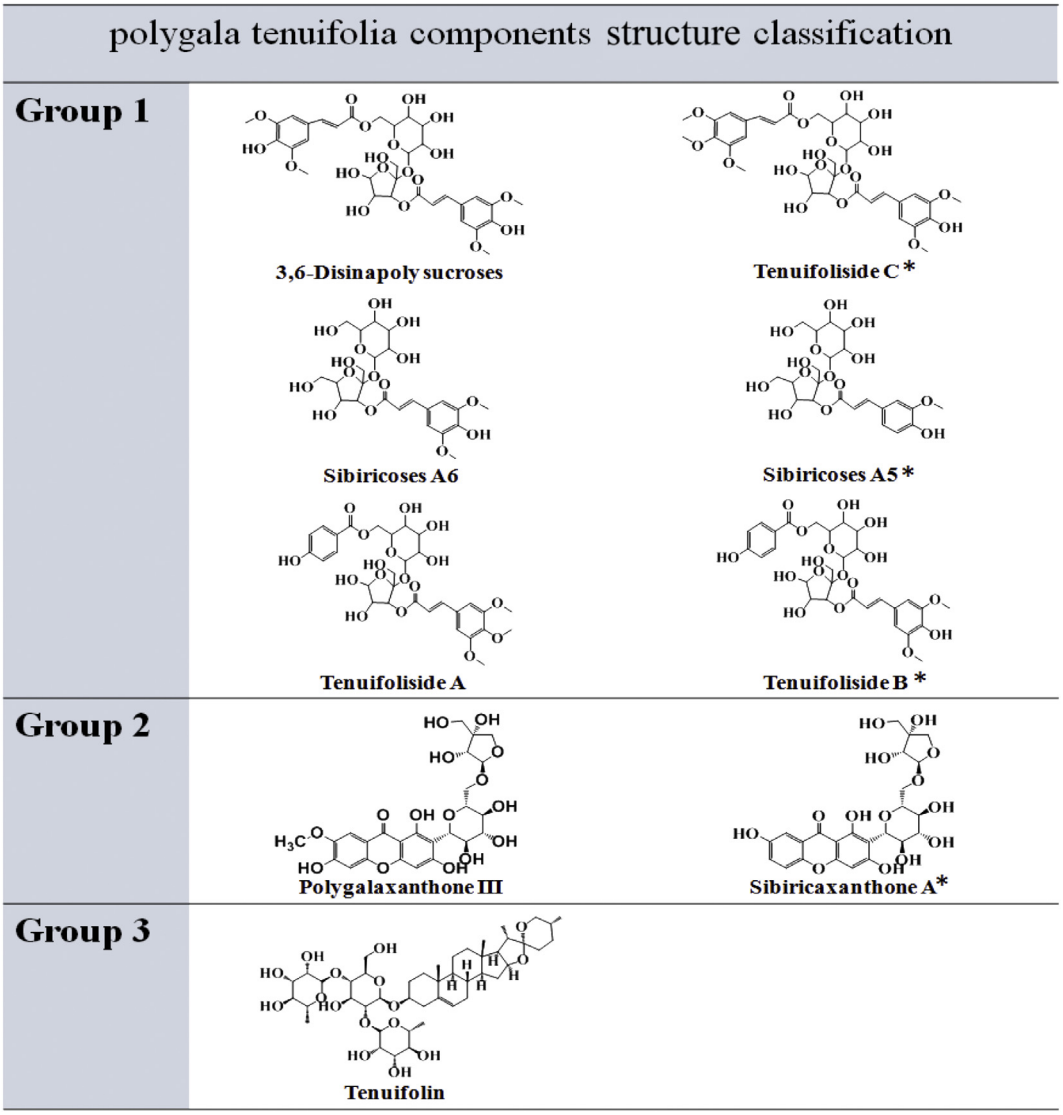

Fig. 3. Matched and preclassified RP components. Components were grouped according to the similarity of structure. Note: * a component lacking reference standard. RP, Radix Polygala.

putatively obtaining the MRM transitions from MS^2 data for the components with LRS is convenient. Optimum CE was determined upon ramping CE at an interval of 2 V range from 20 V to 50 V. Compared with CE, mild variations of Q1 and Q3 have little influence on MS response. Hence, the Q1 and Q3 parameters were adopted according to the same group components. So far, MRM precursor/product ion pairs, as well as the optimum Q1, CE, and Q3 of the components studied, were obtained comprehensively (Table S3).

Taking sibiricoses A6 and sibiricoses A5 as examples, they were classified under the same category because only a methoxy group was observed to be the difference between them. Sibiricoses A6 was infused into the ion source of the TQ-MS for parameter optimization while fragmenting on Q-TOF in MS^2 mode. M/z 205 and m/z 190 were the strongest two peaks in MS^2 which matched well with the product ions optimized in TQ-MS. Similar chemical components with the same fragmentation rules were verified by fragment sibiricoses A5 at a similar mode to that of sibiricoses A6 on the Q-TOF as fragment ion m/z 175 and m/z 160 were obtained. Then, the putative precursor/product ion pairs of sibiricoses A5 were transformed from MS^2 of Q-TOF to TQ-MS. Optimum CE was obtained by stepped comparison on the TQ-MS. In addition, Q1 and Q3 used the same values with sibiricoses A6.

4.4. Semiquantitative methods depend on similar components

The PMRM strategy ingeniously obtained the MRM transitions and the corresponding parameters of RP components with LRS. In addition, a semiquantitative strategy was developed for the quantification of components with LRS when components with ARS were accurately measured according to calibration curves. As previously classified, the concentrations of components with LRS can be calculated in accordance with those of the components with ARS in the same groups. The following equation was applied: LRS components conc. ($\mu g\ mL^{-1}$) = [(LRS components/IS peak area ratio)/(corresponding ARS components/IS peak area ratio)] × corresponding ARS components absolute conc. The implementation of LRS and ARS matching and IS revising, which reduce variability in batches, confirmed the quantification accuracy of those components with LRS.

Then, whether PMRM strategy coupled with the semiquantitative strategy developed can accurately quantify the components comparable with the TMRM strategy coupled with calibration curves

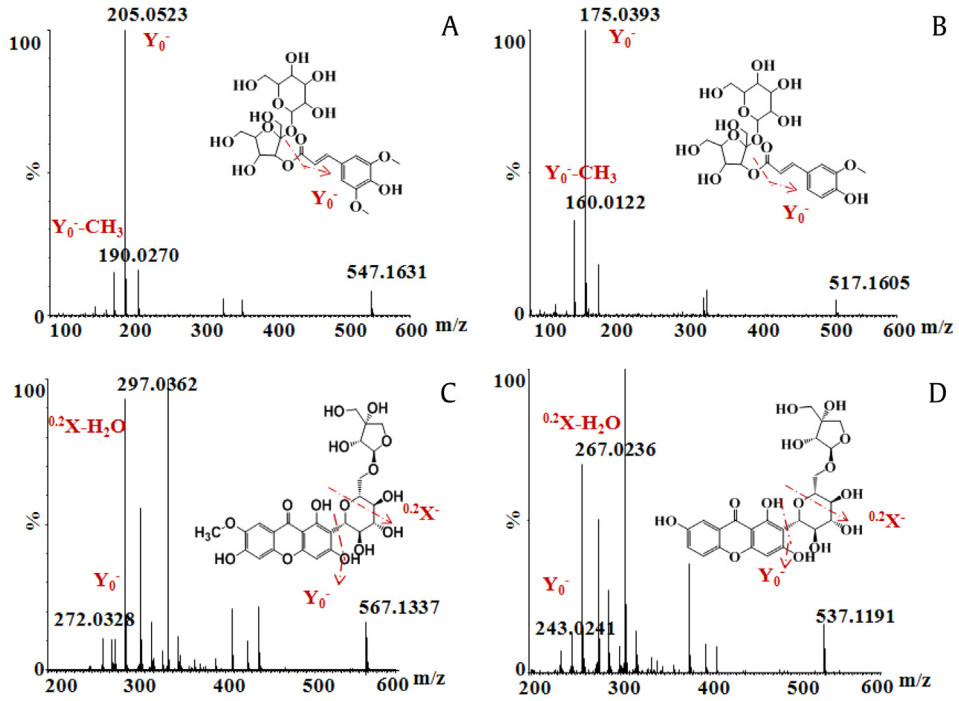

Fig. 4. MS/MS spectra and proposed fragmentation pathways of (A) sibiricoses A6, (B) sibiricose A5, (C) polygalaxanthone III, and (D) sibiricaxanthone A.

dependent quantification method was investigated. To this end, SA6, 3,6-D, and Ta in one group were examined by comparing the experimental values obtained by PMRM and TMRM strategies, respectively. The results of TMRM were obtained by infusion of the standards directly into the ion source of the TQ MS and then quantified using calibration curves, whereas those of PMRM were quantified by semiquantitative strategy dependent on each other under the same group. As Table S4 shows, good agreement and an average absolute error of 5.64% were achieved by the two methods, indicating that PMRM coupled with the semiquantitative strategy developed can be a comparable method to TMRM in the quantification of components with LRS.

5. Method validation

A series of attributes, including specificity, linearity, sensitivity, and so on, were estimated to validate the proposed strategy. All the results met the requirement, and the detailed discussion is presented in the supporting information.

5.1. PK study

PK, the way patients manipulate drugs, is a precondition for a rational therapy. This also holds true for compatibility of TCM because it can help explain the efficacy and toxicity of single herbs and their combinations. Nonetheless, LRS is a bottleneck for quantification because reference standards are prerequisites for PK studies. Therefore, we used the validated PMRM strategy coupled with semiquantitative strategy dependent on the same group components to simultaneously quantify the active ingredients absorbed in the plasma of the TCM extracts. The concentration–time curves of the active ingredients of RG were determined after giving RG or RG–RP extract (Fig. 5). PK solver 2.0 PK software (Chinese Pharmaceutical University) was used to obtain the primary PK parameters in non-compartmental model (Table 1). The PK parameters among the different groups were compared to investigate the possible drug-to-drug interactions. For single RG extract, the five PPD-type ginsenosides, namely, Rb1, Rb2, Rb3, Rc, and Rd, have considerably higher C_{max} and area under the curve (AUC) values than the three PPT-type ginsenosides, Rg1, Re, and Rf. Three possible reasons were mainly summed up as follows. The contents of PPD-type ginsenosides were higher than those of PPT-type ginsenosides, Rg1, Re, and Rf, in the extracting solution per se. In addition, a previous study has reported that PPT-type ginsenoside such as Re has poor intestinal absorption and rapid bile excretion [27]. Moreover, the number of sugar substituent groups was relevant to the absorption rate of ginsenosides [9]. The more the sugar substituent, the slower the rates of absorption and elimination, leading to larger T_{max} value of PPD-type ginsenosides (trisaccharide or tetrasaccharide) than that of PPT-type ginsenosides (disaccharide or trisaccharide).

After oral administration of the Renshen–Yuanzhi extraction, the T_{max} of the active ingredients in the plasma of RG decreased, whereas AUC and C_{max} increased compared with the values of pure RG group. In addition, the elimination rate of RG–RP group was slower than that of pure RG group because $T_{1/2}$ was prolonged remarkably. Moreover, the typical bimodal phenomenon was observed in the RG–RP group, which is remarkably distinguished with the unimodal phenomenon of the RG group. Previous PK study for TCM obtained similar results [28–30]. In conclusion, the mean concentration–time curves and PK parameters of the group almost showed the same trend when compared with the RG group: (1) bimodal phenomenon, which indicates secondary absorption; and (2) better absorption (AUC and C_{max}) and slower elimination rate ($T_{1/2}$), which contribute to higher bioavailability, reflecting the advantages of compatibility. Some possible reasons for these results are as follows. (1) The low bioavailability of RP components was attributed to the faster degradation by the intestinal bacteria than the ginsenosides with larger $T_{1/2}$ values. Hence, in RG–RP compatibility, the competitive inhibition between RG and RP components, which were metabolized by intestinal bacteria, leads to a secondary absorption, resulting in the occurrence of bimodal phenomenon. (2) Previous study has reported that terpenoids can be P-glycoprotein substrates [24]. As triterpenoid saponin, ginsenosides can be P-glycoprotein substrates. In addition, RP

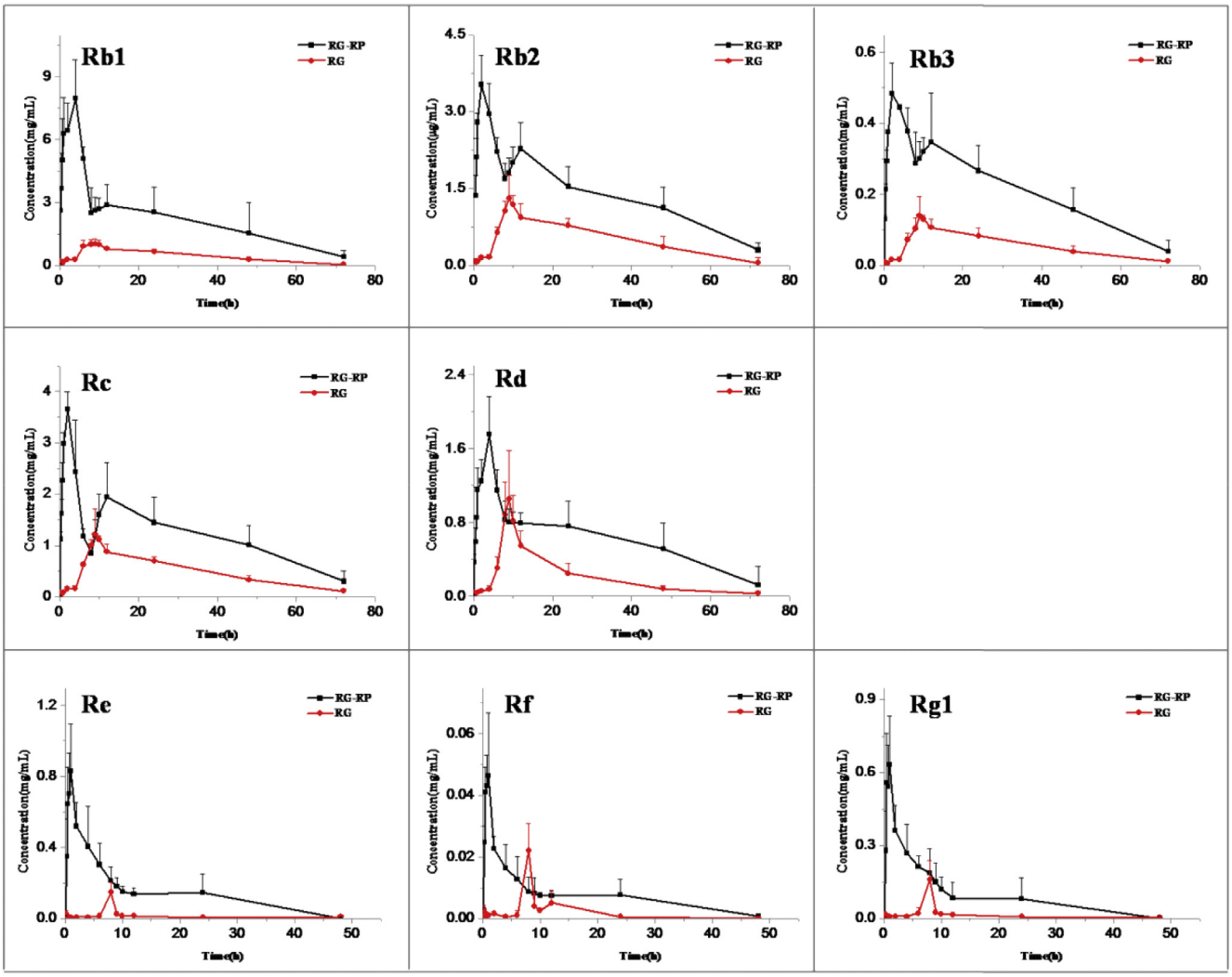

Fig. 5. Comparative mean plasma concentration–time profiles of the active ingredients of RG in rats after i.g. administration of RG and RG–RP extract. RG, Radix Ginseng; RP, Radix Polygala.

ingredients were likely pumped out by P-glycoprotein, which is a drug transporter at the apical membrane [31]. Hence, in the RG–RP group, the competitive inhibition between RG and RP components leads to increased bioavailability, thereby reflecting the synergistic effects of compatibility. (3) Transformation between similar compounds, which appeared very often in PK study with bimodal phenomenon, can be a possible reason for this research [25]. The interconversions between ginsenosides all with sugar substituent were facilitated by RP components because no bimodal phenomenon occurred in the single RG group. Moreover, PPD-type

Table 1
Pharmacokinetic parameters (X ± SD, $n = 6$) of ginsenosides in rat plasma after i.g. administration of RG and RG–RP extract

Analytes	Group	$T_{1/2}$ (h)	T_{max} (h)	C_{max} (μg/mL)	AUC 0-t (μg/mL*h)	AUC 0-∞ (μg/mL*h)
Rb2	RS-YZ	29.20 ± 2.25	2.18 ± 0.25	3.5225 ± 0.1013	102.31 ± 9.566	123.37 ± 9.548
	RS	18.39 ± 1.11	9.25 ± 0.66	1.303 ± 0.0956	37.050 ± 1.569	39.702 ± 1.551
Rb3	RS-YZ	22.75 ± 0.56	2.42 ± 1.24	0.483 ± 0.0833	15.429 ± 0.9622	16.742 ± 0.9634
	RS	18.85 ± 1.56	9	0.1395 ± 0.0345	4.0224 ± 0.1477	4.3488 ± 0.1311
Rc	RS-YZ	23.33 ± 1.23	2.28 ± 0.65	3.653 ± 0.3215	88.164 ± 3.679	98.264 ± 3.711
	RS	19.40 ± 0.94	8.84 ± 0.56	1.2155 ± 0.0953	34.278 ± 2.238	37.357 ± 2.155
Rd	RS-YZ	24.56 ± 2.45	4	1.7555 ± 0.0993	44.948 ± 1.966	48.846 ± 1.836
	RS	15.76 ± 0.16	8.53 ± 2.21	1.0525 ± 0.0122	15.068 ± 0.988	15.751 ± 0.963
Rb1	RS-YZ	17.97 ± 1.41	4.23 ± 1.32	7.96 ± 0.2581	160.22 ± 9.741	170.60 ± 9.644
	RS	15.71 ± 0.88	9.31 ± 0.25	1.013 ± 0.0886	32.065 ± 2.945	33.222 ± 2.951
Rg1	RS-YZ	10.05 ± 0.66	1.32 ± 0.23	0.6327 ± 0.0365	3.9141 ± 0.0647	5.0738 ± 0.0618
	RS	16.66 ± 1.66	8	0.1605 ± 0.0113	0.6633 ± 0.0215	0.7474 ± 0.0220
Re	RS-YZ	5.74 ± 0.75	1.11 ± 0.56	0.8296 ± 0.0584	7.4856 ± 0.5841	7.4967 ± 0.6411
	RS	20.26 ± 1.31	8	0.1465 ± 0.0230	0.6721 ± 0.0266	0.9935 ± 0.0235
Rf	RS-YZ	10.50 ± 0.45	1.83 ± 0.41	0.0463 ± 0.0096	0.3781 ± 0.0452	0.3882 ± 0.0488
	RS	5.03 ± 0.22	8.25 ± 1.23	0.022 ± 0.0012	0.0858 ± 0.0028	0.0895 ± 0.0021

RG, Radix Ginseng; RP, Radix Polygala; RS-YZ, Renshen–Yuanzhi; SD, standard deviation

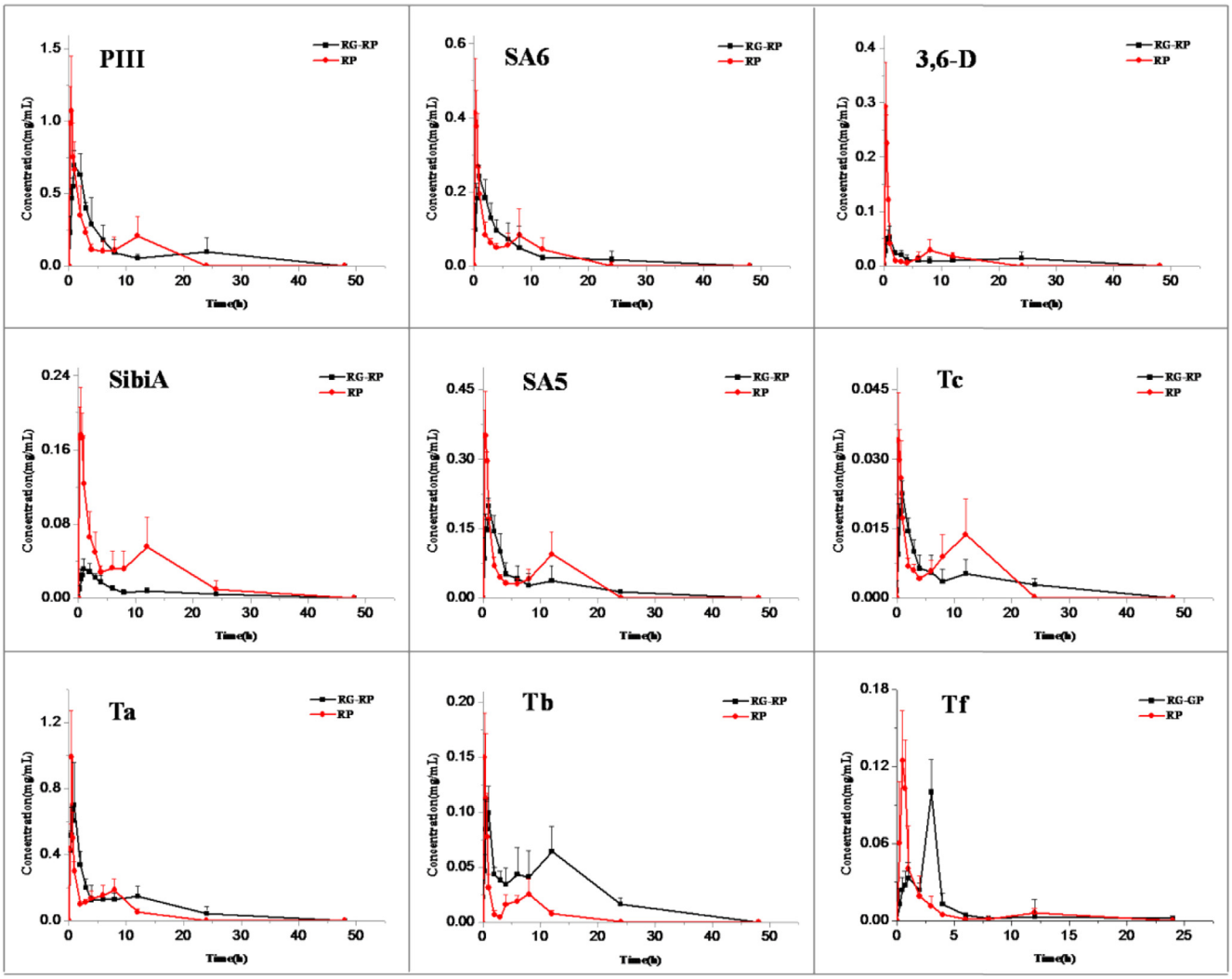

Fig. 6. Comparative mean plasma concentration–time profiles of the active ingredients of RP in rats after i.g. administration of RP and RG–RP extract. RG, Radix Ginseng; RP, Radix Polygala.

ginsenosides exhibited more obvious bimodal phenomena than PPT-type ginsenosides, probably because more sugar substituents are present. RG by itself cannot lead to the interconversions without the promotion of RP.

Similar to the active ingredients absorbed in the plasma of RG, the mean concentration–time curves of active ingredients of RP were determined after oral administration of single-herb RP and RG–RP extract (Fig. 6). Table 2 shows the main PK parameters. In

Table 2
Pharmacokinetic parameters (X ± SD, $n = 6$) of *Polygala* composition in rat plasma after i.g. administration of RP and RG–RP extract

Analytes	Group	$T_{1/2}$ (h)	T_{max} (h)	C_{max} (μg/mL)	AUC 0-t (μg/mL*h)	AUC 0-∞ (μg/mL*h)
SA6	RS-YZ	6.15 ± 0.09	1.15 ± 0.26	0.242 ± 0.0221	1.2982 ± 0.0233	1.4582 ± 0.0213
	YZ	4.19 ± 0.1	0.25	0.4133 ± 0.0122	1.0619 ± 0.1350	1.3357 ± 0.1412
SA5	RS-YZ	11.15 ± 0.11	1.17 ± 0.41	0.1985 ± 0.0065	1.0835 ± 0.0968	1.2939 ± 0.0921
	YZ	2.17 ± 0.05	0.5 ± 0.25	0.3506 ± 0.0315	1.7819 ± 0.0885	1.7820 ± 0.0862
3,6-D	RS-YZ	21.40 ± 0.5	1.42 ± 1.39	0.0533 ± 0.0045	0.3394 ± 0.0251	0.7717 ± 0.0235
	YZ	4.00 ± 0.08	0.25	0.2923 ± 0.0091	0.3623 ± 0.0116	0.4623 ± 0.0119
Ta	RS-YZ	3.48 ± 0.12	0.5 ± 0.11	0.7006 ± 0.0122	1.5117 ± 0.0655	1.7726 ± 0.0641
	YZ	2.85 ± 0.05	1.21 ± 0.43	0.9886 ± 0.0552	4.3608 ± 0.1228	4.3609 ± 0.1233
Tb	RS-YZ	11.95 ± 0.85	1.53 ± 0.26	0.0993 ± 0.0062	1.0721 ± 0.0533	1.3510 ± 0.0526
	YZ	2.58 ± 0.06	0.25	0.1492 ± 0.0051	0.3231 ± 0.0148	0.3243 ± 0.0152
PIII	RS-YZ	7.51 ± 0.23	1.16 ± 1.41	0.6976 ± 0.0082	3.8639 ± 0.1692	4.9190 ± 0.1661
	YZ	2.75 ± 0.22	0.55 ± 0.61	1.0715 ± 0.1011	4.0808 ± 0.3664	4.0847 ± 0.3684
Sibi A	RS-YZ	7.89 ± 1.05	1.61 ± 0.52	0.0315 ± 0.0006	0.2322 ± 0.0199	0.2787 ± 0.0187
	YZ	3.27 ± 0.12	0.5 ± 0.31	0.1760 ± 0.0225	0.9720 ± 0.0458	0.9744 ± 0.0462
Tc	RS-YZ	9.73 ± 1.45	1	0.0226 ± 0.0031	0.1414 ± 0.0211	0.1827 ± 0.0226
	YZ	2.4 ± 0.08	0.25±	0.0341 ± 0.0042	0.2409 ± 0.0155	0.2414 ± 0.0148
Tf	RS-YZ	15.45 ± 1.56	3.45 ± 1.13	0.18 ± 0.0201	0.3445 ± 0.0164	0.3593 ± 0.0157
	YZ	2.171 ± 0.21	0.5 ± 0.12	0.1246 ± 0.0096	0.1531 ± 0.0955	0.1730 ± 0.0945

3,6-D, 3,6-disinapoyl sucrose; PIII, polygalaxanthone III; RG, Radix Ginseng; RP, Radix Polygala; SA5, sibiricose A5; SA6, sibiricose A6; SD, standard deviation; Sibi A, sibiricaxanthone A; Ta, tenuifoliside A; Tb, tenuifoliside B; Tc, tenuifoliside C; Tf, tenuifolin

the RG–RP group, T_{max} and $T_{1/2}$ increased, and C_{max} decreased compared with the single-RP group. An adverse trend was observed in the RG group of T_{max} and C_{max} after combination, whereas a similar trend for $T_{1/2}$ was observed, which all conformed to the competitive inhibition between RG and RP components. Moreover, decreased C_{max} and increased T_{max} attenuated the acute toxic effects of RP components [32,33]. Thus, a preliminary conclusion was drawn, i.e., the TCM formulae were prescribed based on the theory of obtaining synergistic effects and diminishing the toxic effects. And, the penetration is still in progress.

6. Conclusion

In this study, a PMRM strategy, MRM transitions and approximated parameters of which were derived from MS^2 of UHPLC–Q–TOF MS independent on reference standards, was established. The scopes of PK studies were extended by using this strategy. Combined with a group-dependent semiquantification method, sensitive and accurate semiquantification was achieved for components with LRS. The feasibility of the proposed strategy was then successfully exemplified by the PK study of single herbs RG, RP, and their combinations. Visualization results showed that significant differences exist in the PK behavior before and after combination. As expected, the combinations present more advantages, such as prolonged action time and increased bioavailability of medicinal effective components; whereas extended time to peak and decreased concentration for components with dual characters were observed compared with the groups orally administrated with single RG or RP. With the developed PMRM method, the MRM transitions, and relevant PK parameters from the MS^2 mode of UHPLC–Q–TOF MS can be easily obtained for the components with LRS. The developed methodology is expected to be adopted to evaluate the endogenous material for various disease models, and subsequent correlation analysis of pharmacokinetics and pharmacodynamics can be realized.

Conflicts of interest

All authors have no conflicts of interest.

Acknowledgments

This work is supported by the National Natural Science Foundation of China Key Program (No. 81530094) and General Program (Nos. 81573574 and 81873193).

Appendix A. Supplementary data

Supplementary data to this article can be found online at https://doi.org/10.1016/j.jgr.2018.09.007.

References

[1] Shen J, Mo X, Tang Y, Zhang L, Pang H, Qian Y, Chen Y, Tao W, Gou S, Shang E, et al. Analysis of herb-herb interaction when decocting together by using ultra-high-performance liquid chromatography-tandem mass spectrometry and fuzzy chemical identification strategy with poly-proportion design. J Chromatogr A 2013;1297:168–78.
[2] Li Z, Liu T, Liao J, Ai N, Fan X, Cheng Y. Deciphering chemical interactions between Glycyrrhizae Radix and Coptidis Rhizoma by liquid chromatography with transformed multiple reaction monitoring mass spectrometry. J Sep Sci 2017;40:1254–65.
[3] Zhou X, Seto SW, Chang D, Kiat H, Razmovski-Naumovski V, Chan K, Bensoussan A. Synergistic effects of Chinese herbal medicine: a comprehensive review of methodology and current research. Front Pharmacol 2016;7:201.
[4] Yang S, Zhang K, Lin X, Miao Y, Meng L, Chen W, Tang X. Pharmacokinetic comparisons of single herb extract of Fufang Danshen preparation with different combinations of its constituent herbs in rats. J Pharm Biomed Anal 2012;67–68:77–85.
[5] Yang T, Liu S, Wang CH, Tao YY, Zhou H, Liu CH. Comparative pharmacokinetic and tissue distribution profiles of four major bioactive components in normal and hepatic fibrosis rats after oral administration of Fuzheng Huayu recipe. J Pharm Biomed Anal 2015;114:152–8.
[6] Liu R, Gu P, Wang L, Cheng M, Wu Y, Zheng L, Liu Y, Ding L. Study on the pharmacokinetic profiles of corynoline and its potential interaction in traditional Chinese medicine formula Shuanghua Baihe tablets in rats by LC-MS/MS. J Pharm Biomed Anal 2016;117:247–54.
[7] Liu J, Wang JS, Kong LY. Comparative pharmacokinetics of paeoniflorin in plasma of vascular dementia and normal rats orally administrated with Danggui-Shaoyao-San or pure paeoniflorin. Fitoterapia 2011;82:466–73.
[8] Ye H, Zhu L, Wang L, Liu H, Zhang J, Wu M, Wang G, Hao H. Stepped MS(All) Relied Transition (SMART): an approach to rapidly determine optimal multiple reaction monitoring mass spectrometry parameters for small molecules. Anal Chim Acta 2016;907:60–8.
[9] Zhou QL, Zhu DN, Yang YF, Xu W, Yang XW. Simultaneous quantification of twenty-one ginsenosides and their three aglycones in rat plasma by a developed UFLC-MS/MS assay: application to a pharmacokinetic study of red ginseng. J Pharm Biomed Anal 2017;137:1–12.
[10] Lin L, Yin X, Lin H, Li X, Cao S, Qu C, Ni J. Simultaneous determination and pharmacokinetic study of polygalaxanthone III, tenuifolin, tenuifoliside A and tenuifoliside C in rat plasma by LC-MS/MS after oral administration. Analytical Methods 2014;6:6424–31.
[11] Li Q, Zhang S, Berthiaume JM, Simons B, Zhang GF. Novel approach in LC-MS/MS using MRM to generate a full profile of acyl-CoAs: discovery of acyl-dephospho-CoAs. J Lipid Res 2014;55:592–602.
[12] Petritis PC K, Elfakir* C, Dreux M. Parameter optimization for the analysis of underivatized protein amino acids by liquid chromatography and ionspray tandem mass spectrometry. J Chromatogr A 2000;896:253–63.
[13] Nikolskiy I, Siuzdak G, Patti GJ. Discriminating precursors of common fragments for large-scale metabolite profiling by triple quadrupole mass spectrometry. Bioinformatics 2015;31:2017–23.
[14] Luo P, Dai W, Yin P, Zeng Z, Kong H, Zhou L, Wang X, Chen S, Lu X, Xu G. Multiple reaction monitoring-ion pair finder: a systematic approach to transform nontargeted mode to pseudotargeted mode for metabolomics study based on liquid chromatography-mass spectrometry. Anal Chem 2015;87:5050–5.
[15] Liang J, Wu WY, Sun GX, Wang DD, Hou JJ, Yang WZ, Jing BH, Liu X, Guo DA. A dynamic multiple reaction monitoring method for the multiple components quantification of complex traditional Chinese medicine preparations: Niuhuang Shangqing pill as an example. J Chromatogr A 2013;1294:58–69.
[16] Wang EH, Nagarajan Y, Carroll F, Schug KA. Reversed-phase separation parameters for intact proteins using liquid chromatography with triple quadrupole mass spectrometry. J Sep Sci 2016;39:3716–27.
[17] Xu L, Mu LH, Peng J, Liu WW, Tan X, Li ZL, Wang DX, Liu P. UPLC-Q-TOF-MS(E) analysis of the constituents of Ding-Zhi-Xiao-Wan, a traditional Chinese antidepressant, in normal and depressive rats. J Chromatogr B Analyt Technol Biomed Life Sci 2016;1026:36–42.
[18] Attele AS, Wu JA, Yuan C-S. Ginseng pharmacology multiple constituents and multiple actions. Biochem Pharmacol 1999;58:1685–93.
[19] Shin IJ, Son SU, Park H, Kim Y, Park SH, Swanberg K, Shin JY, Ha SK, Cho Y, Bang SY, et al. Preclinical evidence of rapid-onset antidepressant-like effect in Radix Polygalae extract. PloS One 2014;9, e88617.
[20] Tang S, Liu S, Liu Z, Song F, Liu S. Analysis and identification of the chemical constituents of Ding-Zhi-Xiao-Wan prescription by HPLC-IT-MSnand HPLC-Q-TOF-MS. Chinese J Chem 2015;33:451–62.
[21] Feng GF, Liu S, Pi ZF, Song FR, Liu ZQ. Studies on the chemical and intestinal metabolic profiles of Polygalae Radix by using UHPLC-IT-MS(n) and UHPLC-Q-TOF-MS method coupled with intestinal bacteria incubation model in vitro. J Pharm Biomed Anal 2018;148:298–306.
[22] Cruickshank-Quinn C, Quinn KD, Powell R, Yang Y, Armstrong M, Mahaffey S, Reisdorph R, Reisdorph N. Multi-step preparation technique to recover multiple metabolite compound classes for in-depth and informative metabolomic analysis. J Vis Exp JoVE 2014.
[23] Ling Y, Li Z, Chen M, Sun Z, Fan M, Huang C. Analysis and detection of the chemical constituents of Radix Polygalae and their metabolites in rats after oral administration by ultra high-performance liquid chromatography coupled with electrospray ionization quadrupole time-of-flight tandem mass spectrometry. J Pharm Biomed Anal 2013;85:1–13.
[24] Yang B, Liu Z, Wang Q, Chai Y, Xia P. Pharmacokinetic comparison of seven major bioactive components in normal and depression model rats after oral administration of Baihe Zhimu decoction by liquid chromatography-tandem mass spectrometry. J Pharm Biomed Anal 2018;148:119–27.
[25] Li Z, Xiao S, Ai N, Luo K, Fan X, Cheng Y. Derivative multiple reaction monitoring and single herb calibration approach for multiple components quantification of traditional Chinese medicine analogous formulae. J Chromatogr A 2015;1376:126–42.
[26] Liu K, Song Y, Liu Y, Peng M, Li H, Li X, Feng B, Xu P, Su D. An integrated strategy using UPLC-QTOF-MS(E) and UPLC-QTOF-MRM (enhanced target) for pharmacokinetics study of wine processed Schisandra Chinensis fructus in rats. J Pharm Biomed Anal 2017;139:165–78.
[27] Liu L, Huang J, Hu X, Li K, Sun C. Simultaneous determination of ginsenoside (G-Re, G-Rg1, G-Rg2, G-F1, G-Rh1) and protopanaxatriol in human plasma

and urine by LC-MS/MS and its application in a pharmacokinetics study of G-Re in volunteers. J Chromatogr B Analyt Technol Biomed Life Sci 2011;879:2011–7.
[28] Chen ZP, Sun J, Chen HX, Xiao YY, Liu D, Chen J, Cai H, Cai BC. Comparative pharmacokinetics and bioavailability studies of quercetin, kaempferol and isorhamnetin after oral administration of Ginkgo biloba extracts, Ginkgo biloba extract phospholipid complexes and Ginkgo biloba extract solid dispersions in rats. Fitoterapia 2010;81:1045–52.
[29] Wu H, Zhu Z, Zhang G, Zhao L, Zhang H, Zhu D, Chai Y. Comparative pharmacokinetic study of paeoniflorin after oral administration of pure paeoniflorin, extract of Cortex Moutan and Shuang-Dan prescription to rats. J Ethnopharmacol 2009;125:444–9.
[30] Zhu Z, Zhao L, Liu X, Chen J, Zhang H, Zhang G, Chai Y. Comparative pharmacokinetics of baicalin and wogonoside by liquid chromatography-mass spectrometry after oral administration of Xiaochaihu Tang and Radix scutellariae extract to rats. J Chromatogr B Analyt Technol Biomed Life Sci 2010;878:2184–90.
[31] Huang JW L, Zhang L, Luo S, Chen C, Du J. Intestinal absorption characteristics and mechanism of polygala tenuifolia hydrolysate in rats. J Chinese Med Mater 2015;38:556–61.
[32] Yao Y, Jia M, Wu JG, Zhang H, Sun LN, Chen WS, Rahman K. Anxiolytic and sedative-hypnotic activities of polygalasaponins from Polygala tenuifolia in mice. Pharm Biol 2010;48:801–7.
[33] Shin KY, Won BY, Ha HJ, Yun YS, Lee HG. Preclinical safety of the root extract of polygala tenuifolia willdenow in sprague-dawley rats and beagle dogs. Evid Base Compl Alternat Med ECAM 2014;2014, 570134.